

## Condition monitoring approaches for the detection of railway wheel defects

Alemi, Alireza; Corman, Francesco; Lodewijks, Gabri

**DOI**

[10.1177/0954409716656218](https://doi.org/10.1177/0954409716656218)

**Publication date**

2017

**Document Version**

Accepted author manuscript

**Published in**

Institution of Mechanical Engineers. Proceedings. Part F: Journal of Rail and Rapid Transit

**Citation (APA)**

Alemi, A., Corman, F., & Lodewijks, G. (2017). Condition monitoring approaches for the detection of railway wheel defects. *Institution of Mechanical Engineers. Proceedings. Part F: Journal of Rail and Rapid Transit*, 231(8), 961-981. <https://doi.org/10.1177/0954409716656218>

**Important note**

To cite this publication, please use the final published version (if applicable).  
Please check the document version above.

**Copyright**

Other than for strictly personal use, it is not permitted to download, forward or distribute the text or part of it, without the consent of the author(s) and/or copyright holder(s), unless the work is under an open content license such as Creative Commons.

**Takedown policy**

Please contact us and provide details if you believe this document breaches copyrights.  
We will remove access to the work immediately and investigate your claim.

# Review on condition monitoring approaches for the detection of railway wheel defects

Alireza Alemi, Francesco Corman, Gabriel Lodewijks

Faculty of Mechanical, Maritime and Material Engineering (3mE), Delft University of Technology, The Netherlands

Corresponding author:

Alireza Alemi, Faculty of Mechanical, Maritime and Material Engineering (3mE), Delft University of Technology, Mekelweg 2, 2628 CD, Delft, The Netherlands

Email: A.Alemi@tudelft.nl

## Abstract

Condition monitoring systems are commonly exploited to assess the health status of equipment. A fundamental part of any condition monitoring system is data acquisition. Meaningfully estimating the current condition and predicting the future behaviour of the equipment strongly depends on the characteristic of the data measurement stage. Nowadays, condition monitoring has wide applications in the railway industry and various monitoring approaches have been proposed for the inspection of wheel and rail conditions. In-service condition monitoring of wheels provides the real-time data required for maintenance planning, while in-workshop inspection is normally done at fixed intervals carried out periodically. In-service data acquisition can be divided into on-board and wayside measurements. In this paper, on the basis of these classifications, the existing data acquisition techniques for the monitoring of railway wheel condition are reviewed, and the state-of-the-art methods and required research are discussed.

## Keywords

Railway wheel, condition monitoring, data acquisition, in-workshop inspection, wayside measurement, on-board measurement, diagnostic, prognostic,

## Introduction

Wheels are critical components of trains. A comparison between the mechanical components of train, for the years 2004-2007, shows that wheel-set faults by 44.7% are the most important cause of train accidents.<sup>1</sup> Wheels are the subject of numerous defects that consequently influence their smooth revolutions. Eccentricities, discrete defect, periodic non-roundness, non-periodic (stochastic) non-roundness, corrugation, roughness, flat, spalling and shelling are sort of the wheel defects which were reviewed in <sup>2</sup>. These imperfections give rise to high impact forces in the wheel-rail interface, subsequently inducing damage in the rail and train components. Modern trains with faster speeds and larger axle loads have greater wheel-rail contact forces. For this reason, wheel and rail maintenance managers are keen to keep wheels in an adequate condition and detect potential failure as soon as possible. As a result, wheel defect prediction and prevention are essential issues for rolling stock safety and can help to reduce the system-wide maintenance costs.

For a dynamic system such as a railway wheel, there are different ways of estimating the condition: physical modelling, statistical modelling and condition monitoring. Physical models describe the degradation mechanisms of the component or system using a numerical or analytical model. Statistical models collect historical data about failure distribution, for using them in similar systems. The assessment of system features for estimating the

system condition is generally called condition monitoring. Tinga in <sup>3</sup> proposed the concepts of usage and load based maintenance and discussed other methods for condition estimation. In railway systems, some analytical and numerical wheel-rail contact mechanics were reviewed in <sup>4</sup>. For a train with multiple wheels, various environmental situations and operational conditions, such as train speed, acceleration and deceleration, axle load, wheel-rail adhesion, rail profile and track pattern, affect the wheel wear and fatigue parameters and, accordingly, the degradation rate. In addition, the wheel-rail interaction and consequently the degradation pattern varies between the right and left wheels in an axle, from the front to back axles in a bogie as well as from the first to second bogie in a wagon.<sup>5,6</sup> Using numerical, analytical and statistical models is therefore not applicable to in-service wheel condition assessment and accordingly, condition monitoring can be the most convenient method for condition estimation.

A condition monitoring system is usually used to provide a diagnosis of failure for corrective maintenance, in situations where the measured features exceed some predetermined thresholds or show a specific deviation from normal conditions. On the other hand, the data acquired can be used as a prognosis for predicting future failures and the remaining useful life of such wheels. In <sup>7</sup> diagnostic and prognostic approaches, applying condition-based maintenance to different subjects have been reviewed. In <sup>8</sup> the methodology and applications of prognostics and health management design for rotary machinery systems was reviewed.

Condition monitoring has wide applications in the railway industry. In <sup>1</sup> and <sup>9</sup> the applications of monitoring systems for train equipment such as wheel-sets, bearings, suspensions, overhead lines and car bodies were reviewed. Previously, the recognition of faulty wheels was done by way of visual inspection at fixed times.<sup>10</sup> Since 2007, in the Netherlands the wheel maintenance policy by NedTrain was based on the preventively machining; a condition monitoring system has been used to detect unexpected failures.<sup>11</sup> Optimizing the maintenance plan for wheels based on the prognosis of possible future failures according to condition monitoring data can be more efficient.

An essential step in any condition monitoring process is data acquisition. Assessing the current condition and forecasting the future condition is strongly depending on the measurement stage. Condition monitoring is based on the fact that certain features and indicators express the degradation of a system in 99% of all failures.<sup>12</sup> Hence, selecting an adequate sensor type for measuring and processing these features is vital. A data acquisition system can measure directly the failure features, and indirectly the failure effects.<sup>13</sup> For railway wheel monitoring, some sensors are used to assess the existence of cracks and abnormalities directly on the wheels and, differently, some sensors are used to measure the output of faulty wheel interaction with the rail, based on acoustic, vibration and strain effects.

Generally, based on <sup>14</sup>, data acquisition approaches in the railway industry can be classified into the following four groups: infrastructure-based infrastructure monitoring, infrastructure-based rolling stock monitoring, rolling-stock-based infrastructure monitoring and rolling-stock-based rolling stock monitoring. Data acquisition for the monitoring of railway wheels can be reviewed from different angles. In-service and in-workshop inspection, wayside and on-board measurement and diagnostic and prognostic approaches are worthy examples. Barke and Chiu in <sup>15</sup> have reviewed the application of wayside detection systems in the railway industry up to 2005. Among those wayside detectors, there are some systems that are relevant to wheel conditions such as strain-based wheel impact monitors, accelerometer-based wheel impact monitors, mechanical profile monitors, wheel profile detectors and cracked wheel detectors.

In this paper, the available condition monitoring approaches to the detection of railway wheel defects are described. The data acquisition systems are divided into in-workshop and in-service inspection, then in-service inspection is divided into on-board measurement and wayside measurement. So, the relevant literature is categorized based on sensor type. Finally, the measurement objectives, the measurement conditions and diagnostic and prognostic approaches are discussed.

## **In-workshop inspection**

Railway wheels are regularly inspected at workshops in their short and long periodic phases. The assessment of hundreds of wheels in a day requires appropriate equipment to test multiple wheels mounted under the trains.

These evaluations should map the existence of cracks and defects in different parts of wheel such as on the surface, below the surface (sub-surface), on the flange and disk. Several methods have recently been developed for this purpose. In this section, the available workshop methods for the inspection of railway wheels are discussed according to the various data acquisition approaches.

### *Ultrasonic techniques*

At present, ultrasonic techniques are being intensely used for non-destructive evaluation. Drinkwater *et al.* in <sup>16</sup> reviewed the ultrasonic arrays technique as non-destructive evaluation and discussed its relevant array design, modelling and signal processing. The ultrasonic method is one of the main non-destructive tests usually used in the railway industry to evaluate rolling stock, during manufacture procedures and maintenance inspections.<sup>17</sup>

Pohl *et al.*<sup>18</sup> exploited ultrasonic inspection techniques for sub-surface cracks of the wheel. From the end-user's point of view they carried out the inspection without disassembling the wheels. To this end, they designed a multi-probe holder with 14 shear wave probes and three straight beam probes, as shown in Figure 1. The intensity of the shear waves and the angle of incidence depend on the complex wheel geometries for detecting tangential oriented defects and radial defects in different areas of the wheel disk. This method requires two turns of the wheel for assessment. The first rotation of the wheel is for wetting the tread and the next one is for the ultrasonic inspection.

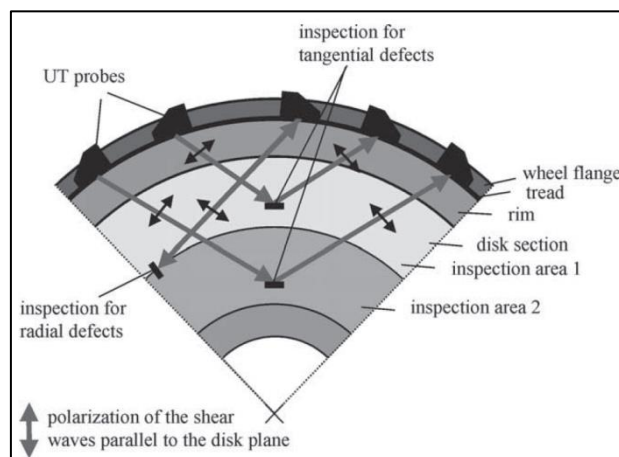


**Figure 1.** The schematic view of the shear wave probe arrangement.<sup>18</sup>

Pau in <sup>17</sup> explored the possibility of applying ultrasonic waves to diagnose faults in the wheel–rail contact interface. The contact conditions are evaluated by analysing the acquired amplitude of the wave reflected by the contact interface. This is based on the fact that the reflection coefficient in the actual condition is partially dependent on the force exerted. In laboratory tests, some artificial defects were created on two types of rails and three types of wheels. Wheel and rail samples were then loaded up to 10kN. The ultrasonic probe was immersed in water at the proper distance to simply focus on the contact region. The results of these laboratory experimental investigations showed that the ultrasonic technique could be used to assess wheel-rail contact irregularities. Furthermore, this provides sufficient evidence on certain important contact parameters such as size, the shape of the nominal contact area, the real contact area, and contact pressure. These tests were done in the laboratory and in stationary conditions. The layout of the rail, wheel and ultrasonic probe is displayed in Figure 2 and the wheel-rail contact maps for different examinations are shown in Figure 3. Pau *et al.* in <sup>19</sup> developed their processing method to investigate the sub-surface cracks.

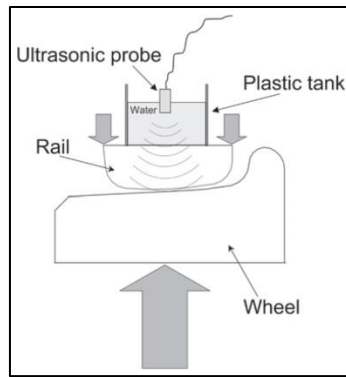


**Figure 2.** A schematic of the components for wheel–rail contact ultrasonic analysis.<sup>17</sup>

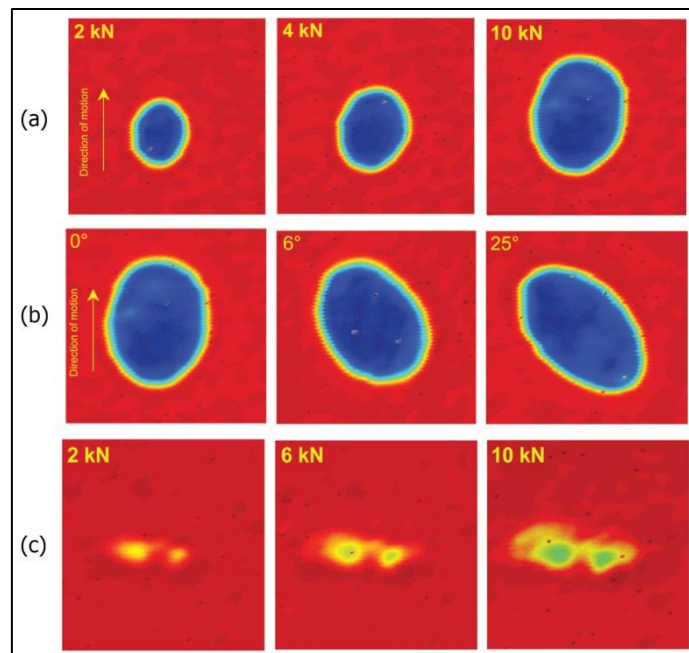


**Figure 3.** (a) normal wheel-rail contact and its evolution by increasing the load, (b) misaligned wheel-rail contact, (c) irregular contact because of the defective wheel.<sup>17</sup>

Fatigue and wear analysis for defining and predicting the lifetime of any wheel and section of rail depends on the determination of the interface pressure in wheel-rail contact. Damage leads to restructuring the contact stresses. Marshall *et al.* in <sup>20</sup> used ultrasonic techniques to assess the stress and pressure distribution in different wheel-rail conditions such as new, worn and damaged. The reflection of an ultrasonic wave in a wheel-rail interface was modelled as a spring. This model was applied to draw maps of contact stiffness based on wheel-rail ultrasonic reflection data. Ultrasonic measurements for contact pressure distributions were compared to Hertzian smooth elastic, elastic models and elastic-plastic models and it was found that ultrasonic results are generally correlated to numerical models.

Peng *et al.* in <sup>21</sup> described phased array ultrasonic techniques for the static assessment of railway wheel-sets in the workshop. This method uses composite crystal as a phased array to produce ultrasonic waves. It is a suitable technique for finding surface and sub-surface cracks in the wheel rims and disks. For this purpose, the wheel-set should be disassembled from train. They explained the lifting and rotating system structure and the arrangement of the ultrasonic probes. Developing a data processing algorithm for the automatic analysis of the ultrasonic data is the subject of another paper produced by their group.<sup>22</sup> This process detects and localizes the wheel faults in the ultrasonic image.

### ***Infrared camera***

The use of an infrared camera to detect cracks in a railway wheel is based on the difference in the thermal conductivities of steel and the air layer in the crack. Any thermal resistance of cracks to heat flow leads to rapid changes in the temperature of the crack area. Verkhoglyad *et al.* in <sup>23</sup> recorded the alteration of the temperature extension on the surface of the wheel disc by means of an infrared camera. Contrary to the worthy results for recognizing the sub-surface cracks, this method can only be performed in workshops. In addition, it is an active method that requires heating. Furthermore, the crack is detectable about 3 min after starting the heating process. Hence, it is not suitable for in-service implementation. Another matter that arises in relation to the use of the thermal imager and an infrared radiation camera involves selecting the operation range of wavelengths.

### ***Magnetic methods***

Exerting an alternating current on an induction wire provides an electromagnetic field around the neighbouring region. Approaching this electromagnetic field with a conductive metal creates a current in the conductive metal. Assessing the potential drop related to this sort of derived current is the basis of the induced current focusing potential drop technique discussed in <sup>24</sup>. Several artificial railway wheel defects were applied and then this method was used to detect the surface and sub-surface cracks. These non-destructive tests show that induction wires (of about 40 mm in length) must be positioned at a certain distance from the crack (5 mm distance) to be able to detect the cracks. Then the pick-up pins and induction wire must be reordered to an orientation perpendicular to the crack initiation position; hereafter these make it challenging for practical applications.

Because of its depth, detecting fatigue damages is challenging and the monitoring of fatigue damage in the wheel is important because of its abrupt fraction. Zurek in <sup>25</sup> used permeability and coercivity for monitoring of fatigue damage. He assessed the alteration in a coefficient defined by these magnetic properties. This coefficient is a function of plastic or fatigue deformations and the number of fatigue cycles. In Figure 4, the results of the circumferential monitoring of a railway wheel are displayed. The fatigue damage at 120° is clearly observable.

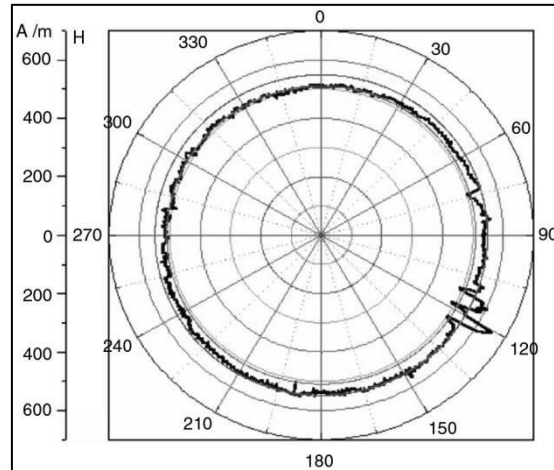


**Figure 4.** Circumferential plot of a magnetic assessment.<sup>25</sup>

Hwang *et al.* in <sup>26</sup> used an array of linearly integrated Hall sensors to make a magnetic camera for the detection of wheel tread defects. The layout of the system is shown in Figure 5.

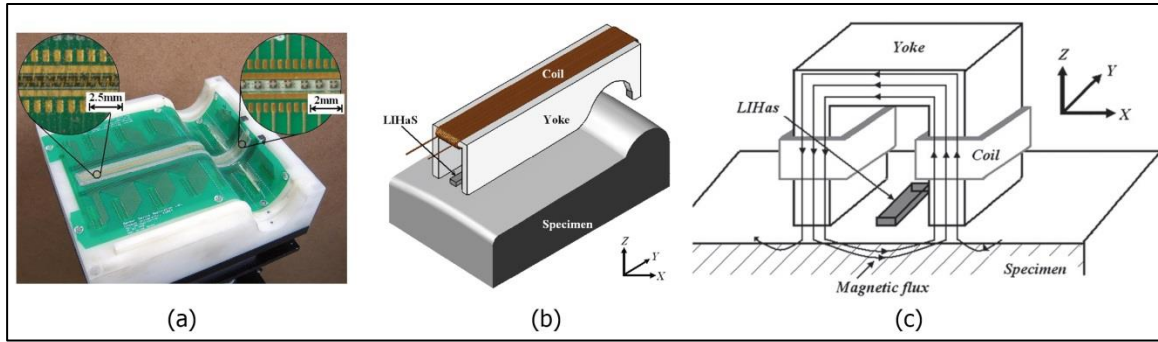


**Figure 5.** (a) Hall sensor array on a wafer<sup>27</sup>, (b) and (c) yoke-type electromagnetic coil.<sup>26,27</sup>

This magnetic camera measures the Hall voltage in every area of the wheel tread. Because of crack existence, the alteration of the voltage between the sensors ( $\partial V_H / \partial x$ ) is plotted to directly achieve the crack information. The selection of an adequate cut-off frequency is necessary for finding an optimum signal-to-noise ratio and signal resolution. The authors ran a laboratory test to evaluate this technique for detecting the surface cracks and the results of differential-type of magnetic camera are shown in Figure 6.

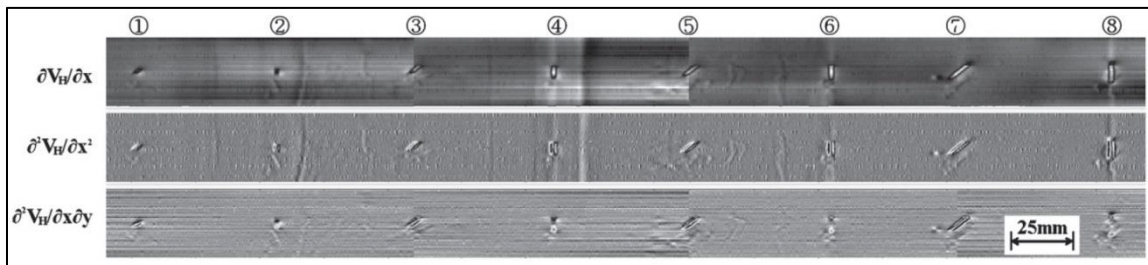


**Figure 6.** Eight surface cracks on a specimen of wheel and the results of the differential-type magnetic camera.<sup>26</sup>

## In-Service measurement

Railway operators, owners and maintainers want to know the real-time conditions of trains and infrastructures. The unexpected failure of critical components such as wheels disrupts normal operations and in the worst cases leads to derailment. Hence, in-service monitoring of wheels has been the subject of much research in recent decades. In-service monitoring of wheel can be categorized as on-board and wayside measurements. On-board measurement implies methods that install sensors on the train. In spite of offering continuous and comprehensive data from the system, this aspect is generally inherently complex in terms of mounting, implementation and maintenance. On the other hand, wayside approaches attempt to measure the wheel features by installing sensors on the rails and surrounding areas. Such indirect and discontinuous measurements tend to give limited information about wheel condition while they can monitor multiple trains and wheels with only one sensor. In this section, the available measurement techniques for on-board and wayside measurements are reviewed.

### *On-board measurement*

One approach to wheel condition monitoring is to install a sensor on the wheel or on the vehicle. These methods usually require specific equipment for mounting the sensors. In<sup>14</sup> the applications of sensors mounted on trains to monitor the condition of rails and rolling stock were reviewed. Magnetic, ultrasonic, acoustic and vibration techniques are the sorts of methods that are discussed.

**Magnetic technique.** The ratio of the lateral and vertical contact forces is called the derailment coefficient. This coefficient is traditionally measured by particular wheel-sets equipped with strain gauges. Matsumoto *et al.*<sup>28</sup> used non-contact gap sensors to measure the wheel-rail contact forces on a test rig and on a commercial line. The authors measured the lateral contact force from the lateral bending of wheel by means of a non-contact

gap sensor. This method is used instead of the equipped wheel-sets method because of its expense, hardwearing quality and simplicity in usage. In Figure 7, the configuration of such non-contact gap sensors is showed.

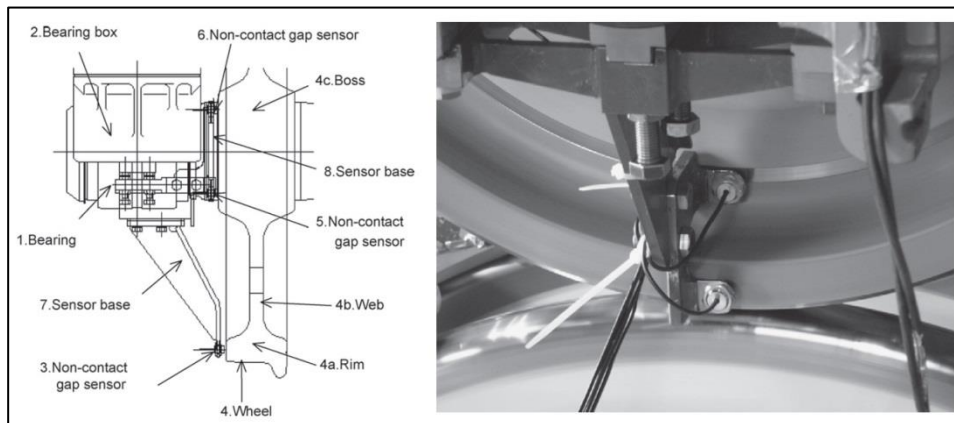


**Figure 7.** Arrangement of gap sensors for lateral force measurement.<sup>28</sup>

They expanded their research in <sup>29</sup> by implementing the method suggested in <sup>28</sup> for continuous measurement of the contact forces and derailment coefficients at different curves of commercial lines by using in-service trains. They assessed several factors such as friction and track irregularity, which are effective for the alteration of derailment coefficients. As a result, the extreme derailment coefficients are obtained at the same point in the track curve since the shapes of the line are fixed during measuring.

**Ultrasonic techniques.** In <sup>30</sup> several simulations and laboratory tests were accomplished to study the possibility of mounting the ultrasonic sensor on the wheel. Riding the sensors on the wheel prepares dynamic data for flange contact. When the ultrasonic pulse impacts an identical interface by means of full contact, the signal will be completely transmitted. These simulations and laboratory tests measured the proportion of the reflected and transmitted ultrasonic pulse from no contact to perfect contact. In simulation modelling, they determined the perfect position for the ultrasonic transducer on the wheel. In experimental tests, they loaded sections of wheels and rails by means of a bi-axial frame to produce different wheel-rail contact conditions. They believe that the full-scale wheel-rail rig is a good idea for the next stage.

**Acoustic technique.** A simulation and laboratory test based on acoustic sound produced by faults on the wheel tread was developed in <sup>31</sup>. In that work, a sensor was located inside the hollow shaft of the wheel-set axis. The elastodynamic finite integration technique was used to simulate ultrasonic sound propagation. Different artificial cracks were exploited for laboratory testing by bearing in mind that crack width affects signal length and severity.



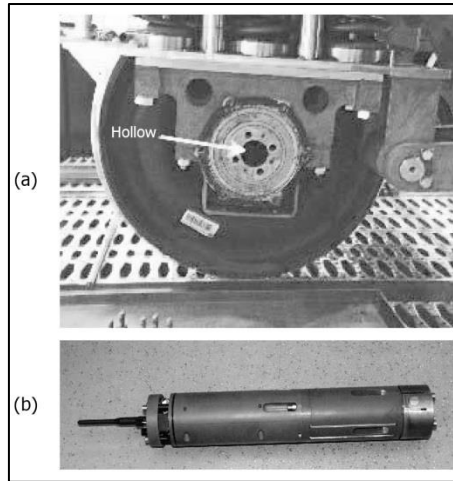


**Figure 8.** (a) Hollow shaft in wheel-set (b) integrated condition monitoring system.<sup>31</sup>

**Vibration technique.** Liang *et al.* in <sup>32</sup> prepared a simplified mathematical model and a simulation of the wheel flat and rail surface defects. Afterwards, the test results of vertical forces and accelerations obtained from a roller rig were compared with this simulation. Five accelerometers were mounted on the roller rig. Displacement and velocity were computed by integrating vertical axle box acceleration. Analysis of vibration and acoustic signals was carried out with different time domain techniques such as the Crest factor, Skewness, RMS and peak values as well as time-frequency techniques such as the short-time Fourier transform, the Wigner–Ville transform and the wavelet transform. When the wheel speed was increased from 3.5 km/h to 15 km/h, the differences between the simulation and experimental results of the wheel accelerations emerged. Their research was extended by concentrating on noise elimination and time-frequency analysis to improve the results acquired in <sup>33</sup>. They assessed the performance of adaptive noise cancelling as a pre-processing method and looked at four time–frequency transforms as processing methods including smoothed pseudo Wigner-Ville transform, the short time Fourier transform, the Choi-Williams transform and the wavelet transform on the raw measured acceleration signals. These tests, like prior work, were carried out at a low speed hence they are not suitable for real field application. In Figure 9, a 1/5 scale roller test rig is displayed.



**Figure 9.** Scaled roller test rig.<sup>32</sup>

Jia and Dhanasekar in <sup>34</sup> carried out a simulation to evaluate the ability of two wavelet methods when exploiting the vertical acceleration signal of the bogie to identify the wheel flat. These approaches involve average signal wavelet decomposing and wavelet local energy averaging. Selecting the convenient wavelet function is important for the detection process; therefore, the authors tried five different types of wavelets and selected the Daubechies wavelets as the best one.

### ***Wayside measurement***

Wayside measurement is the monitoring of train equipment by means of sensors that are mounted on the rail or along it. The preliminary model of the wayside wheel defect detector was built in 1983 and attached to the North East Corridor between New York and Washington to measure the wheel impact load and detect faulty wheels.<sup>35</sup> The wayside system rapidly became a widespread device for wheel monitoring. For instance, in Sweden the first wayside detectors were installed in 1996 and now more than 190 wayside systems are working.<sup>36</sup>

Some wayside detectors investigate the wheels to directly find cracks and defects, while others concentrate on failure features. The wheel and rail characteristics create the wheel-rail contact behaviour. If we know the current condition of the rail, we will indirectly discover the condition of the wheel by monitoring the different wheel-rail contact features such as acoustics, vibration and strain. In this section, wayside detection systems for monitoring of railway wheels according to their measurement approaches are discussed.

***Strain gauges.*** Measuring the surface defects by means of strain gauges is a conventional and commercial technique for the wheel condition monitoring. Some examples of present commercial products that are available are mentioned in <sup>37</sup>. The passage of any train causes deviations in rail strain and it is alteration that gives rise to variations in the resistance of the strain gauge sensors. Through this method, the strain gauges are welded to the rail to measure the impact force caused by wheel defects. The position, number and arrangement of these sensors are determined according to the purpose and situation of measurements.

Stratman *et al.* in <sup>38</sup> exploited the data acquired from a wheel impact load detector to indicate the defective wheels. The wheel impact load detector was equipped with 128 welded strain gauges. This system measures the vertical force by means of two strain gauges and the lateral force by means of other two strain gauges at each point. Therefore, it gathers the vertical and lateral forces at 16 points per rail. This distribution covers 90% of the circumference of the wheels in different sizes. A schematic overview of the rail web with the installed strain gauges is shown in Figure 10.

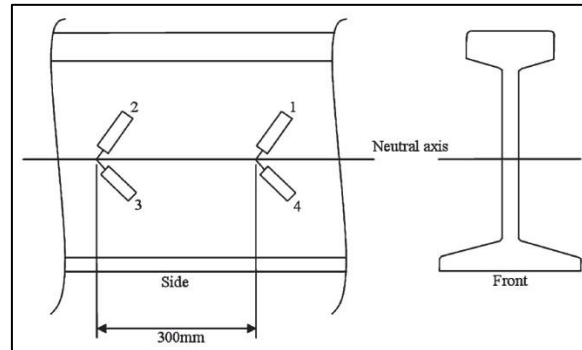


**Figure 10.** Configuration of strain gauges on the web of the rail.<sup>38</sup>

Usually the average and the maximum of the measured vertical force are used as features of the faulty wheels. The authors in <sup>38</sup> suggested two indicators based on statistic trends of vertical force, in order to detect the wheels with high probability of failure. These indicators assess the trends of rapid increase in vertical force during a particular period (within 50 and 20 days) for two groups of wheels. First, wheels with high dynamic impact force (this high impact load is lower than threshold) and second, wheels that are running at a normal impact. Based on these methods, 15.8% of the wheels in North America were eliminated because of their high probability of failure while their impact forces were lower than threshold limit.

Palo *et al.*<sup>6</sup> measured lateral wheel-rail forces by the strain gauges to assess the effect of the wheel position in a bogie on the lateral forces. This assessment was carried out in a 484 m radius curvature at a specific research station. The trains operated within a speed range up to 100 km/h and severe weather situations such as snow and temperature variation between  $-40^{\circ}\text{C}$  to  $+25^{\circ}\text{C}$ . In <sup>39</sup> they exploited high-speed cameras and lasers for the wheel

profile features monitoring and used the wheel-rail forces to decide for the wheel maintenance. The fusion of these two pieces of data about the wheel condition, gives useful information for maintenance decision making.

**Fibre Optic Sensing Technology.** A Fibre Bragg Grating (FBG) sensor is created by exposing a short section (around 1 cm<sup>40</sup>) of an optical fibre to ultra-violet (UV) radiation over a phase mask, in a way that mask pattern creates a periodic refractive index.<sup>10</sup> The light in an optical fibre travels freely while the FBG sensor reflects back a specific wavelength of the light spectrum relating to the Bragg feature.<sup>40</sup> The mechanism of FBG sensors is based on the fact that the changing in mechanical and thermal stress leads to change in refractive index of the FBG sensor and this alteration leads to the change in the wavelength of the reflected light spectrum which is detected by means of an optical interrogator. This operation is illustrated in Figure 11.

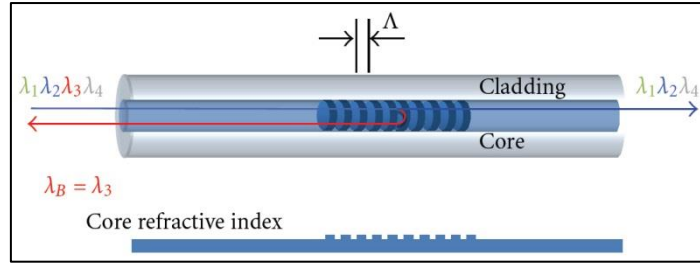


**Figure 11.** Schematic view of a FBG sensor and the reflected light.<sup>40</sup>

The reflected back wavelength ( $\lambda_B$ ) is calculated according to:

$$\lambda_B = 2n_e\Lambda \quad (1)$$

In this equation,  $n_e$  is the refractive index of the core and  $\Lambda$  is the grating period of the FBG sensor. The alteration of the reflected wavelength ( $\Delta\lambda_B$ ) shows a nearly linear relation to the alteration of the strain and temperature, which are respectively  $\sim 1\text{pm}/\mu\epsilon$  and  $\sim 11\text{pm}/^\circ\text{C}$ . The wavelength shift can be measured by two common methods: wavelength-division multiplexing and time-division multiplexing, which are used in interrogating system.<sup>41</sup>

Lee *et al.* in<sup>42</sup> applied FBG to assess the derailment probability. The weight of the train is useful for assessing the off-loading ratio that is a parameter related to the probability of the train derailment:

$$\text{Off-loading ratio} = \frac{\Delta Q}{Q} = \frac{(Q_1 - Q_2)}{(Q_1 + Q_2)} < 0.6 \quad (2)$$

$Q_1$  and  $Q_2$  are the vertical forces of the wheels in a wheel-set. This means that the transferred load in one axle should be limited to 60%. In addition, they remarked the ability of FBG sensors for axle counting, train identification and speed detection.

In<sup>40</sup> their group used Fibre Bragg Grating sensors to measure the weight of trains in a commercial railway line. Furthermore, they evaluated four methods to correlate the weight of axles to the measured data:

$$W1 = (P1 - V1) \quad (3)$$

$$W1 = (P1 - V2) \quad (4)$$

$$W1 = (P1 - (V1 + V2)/2) \quad (5)$$

$$W1 = P1 \quad (6)$$

According to Figure 12,  $P$  and  $V$  are the maximums and minimums of the measured signal respectively. The authors concluded that the most accurate method is the equation 6 with the smallest amount of error.<sup>40</sup>

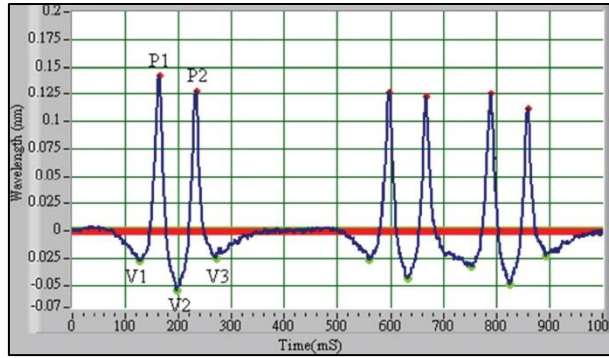


**Figure 12.** A typical output of a FBG sensor which shows strain changes during the passage of a train.<sup>40</sup>

Tam *et al.*<sup>41</sup> applied around 30 FBG sensors to measure the train speed. The speed of the train is calculated using the time it takes for passing two axles over sensors (two peaks), considering that the distances between the axles are known. The details of measurement condition and sensors array were not discussed.

Wei *et al.*<sup>43</sup> used FBG sensors to count the axles, which pass the sensors. The main problem here is the processing of noisy signals. The faulty wheels create an impact on the rails and make some extra peaks in the strain signals. The authors proposed two approaches to solve this problem, named X-crossing and D-crossing. Combination of these two methods presented 100% successful rate of axle detection. In<sup>10</sup> they fabricated a packaged FBG sensor and proposed a condition index to quantify the wheel condition. For their field examination, the FBG sensors were mounted neighbouring the rail foot. These sensors were linked through optical cables in series. They applied high-pass and low-pass filtered and Fast Fourier Transform to analyse the acquired data. Figure 13 illustrates the strain variation obtained from one FBG sensor induced by a passing train with 12 cars and 48 axles, with speed between 50-90 km/h.

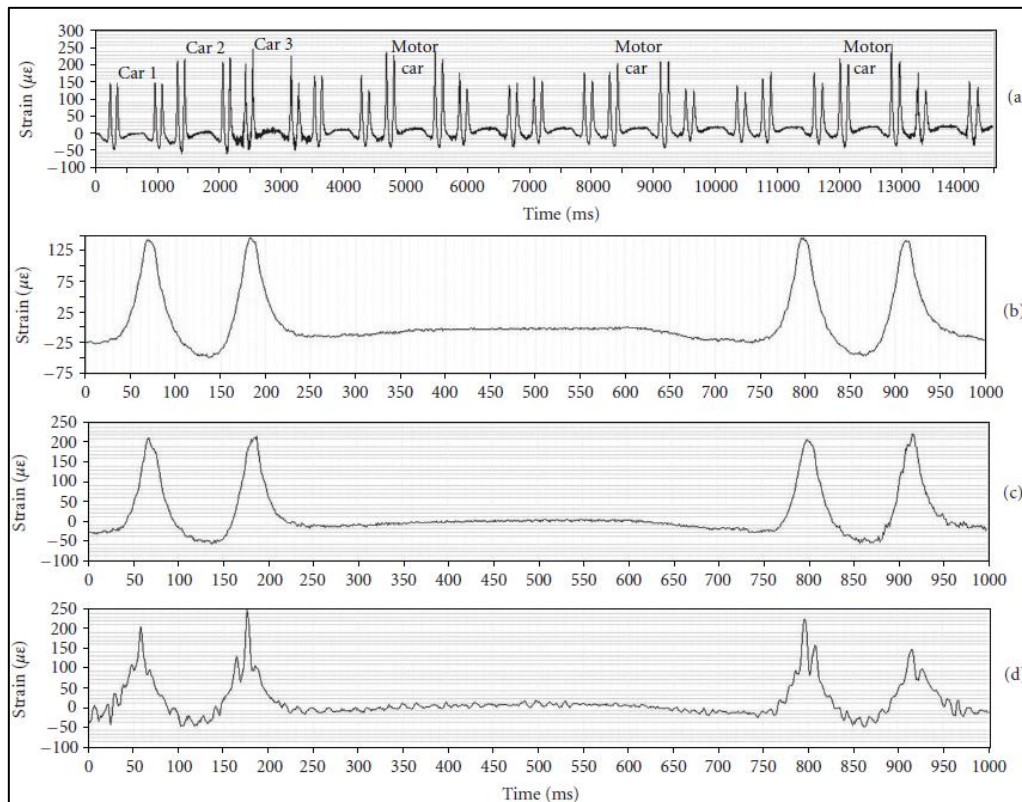


**Figure 13.** The strain change by means of (a) a train passage, (b) the first car that is smooth, (c) the second car that is a little out-of-round, (d) the third car that is highly out-of-roundness.<sup>10</sup>

Filigrano *et al.* in <sup>44</sup> installed 22 FBG sensors (11 per track) on the straight part of a rail in various positions to monitor the different types of high-speed trains. The speed of trains in that sector is usually between 200–300 km/h. They measured the environment temperature and rail strain change to determine the train speed and acceleration, axle numbers, train category recognition, dynamic load, and the wheel imperfections. An array of these 11 FBG sensors is displayed in Figure 14.

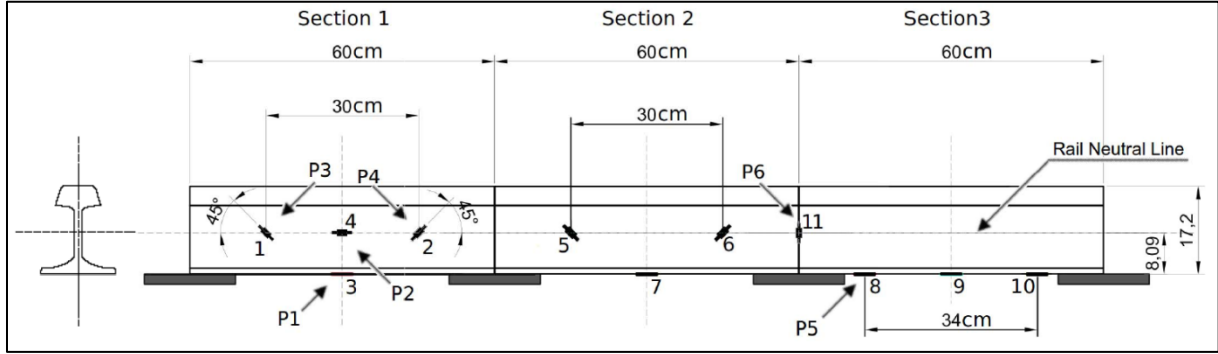


**Figure 14.** Six positions of 11 FBG sensors (P1-P6) located on the rail. <sup>44</sup>

This system continuously measures, while only storing the data that contains the passage of train. For the axle counting, they measured fast change in the signal to find the number of peaks. For the train type identification, they matched the number of counted axles with prior information from the trains, like the axle distance for different types. By using the time intervals between the peaks in a wagon, instantaneous speed is calculated. For estimating the average speed of the train, the data of the first and the final wheel of a train are used. For measuring the acceleration of the train, the obtained speed of the first and the last wagons are exploited. The vertical impact load can be measured by means of shear strain, obtained by P3 and P4 sensors, and the rail characteristics based on the below equation:<sup>44</sup>

$$Q_{xz} = \frac{2\varepsilon_{xz}GbGI_y}{S_y} \quad (7)$$

It means that the vertical load ( $Q_{xz}$ ) is proportional to the differential shear strain ( $\varepsilon_{xz}$ ), the tangential elasticity module ( $G$ ), the width of the section in the rail neutral line ( $b_G$ ), the inertial momentum of the section ( $I_y$ ), and inversely proportional to the static momentum of the lower part of the rail ( $S_y$ ). In some cases the calculated vertical impact load based on this method were slightly higher than the static load, and in some cases equal or even lower than the static load, hence calibration of this method is required.<sup>44</sup>

Filigrano *et al.* in <sup>45</sup> provided the same condition monitoring system <sup>44</sup> using FBG sensors to perform the field tests. They focused on the detection of out-of-roundness, the calculation of the impact force, the estimation of the static load and the discrimination between close flats in the case that the train contains several defective wheels. The first step of their offline processing was applying a high-pass filter. The envelope of the high-pass filtered signal derives the energy of the signal. A time-frequency analysis of the signal was used for the defective wheel detection. In order to distinguish between several wheel flats they assessed three different scenarios based on phase matching between close-flatted wheels. For assessing the static load, they used the interpolation estimate of the average value of the dynamic load. In the preceding work <sup>44</sup> the authors had calibration problem in the calculation of the dynamic load, hence they added coefficient  $k_c$  which is equal 1.34.

Pan *et al.* <sup>46</sup> designed a structure for installing the FBG sensor to increase the sensitivity of the vertical wheel-rail force measurement. For achieving this purpose, they positioned the FBG sensor in the centre of a thin steel gauge and suspended the fibre from its two ends. It means that the glue does not cover the whole of fibre. This scheme prevents FBG chirping and increases its sensitivity in a ratio of 1.7 to the measurement of the direct installation. They used an array of 24 sensors, covered 6.6m, to monitor the whole circumference of the wheel.

For calculating the sensitivity, they used a standard weight locomotive. This sensitive coefficient is valuable for calibrating the measured FBG wavelength which is used for detecting the dynamic wheel load.<sup>46</sup>

**Ultrasonic Technique.** Salzburger *et al.*<sup>47</sup> proposed a wayside and in-service monitoring system to evaluate the wheels, for finding surface cracks, based on ultrasonic inspection. This system contains two special patented probes (EMAT) per rail and a particular track for installation of the probes. As a result, monitoring is limited to specific stations; also, the trains speed is restricted to 15 km/h. Every sensor is able to completely assess the circumference of the wheel and the second sensor is only used for double inspection. As other typical ultrasonic inspections, this system relies on pulse-echo and pulse transmission, but it does not need liquid couplings. In addition, it emits waves in circumferential orientation for observing the surface and sub-surface cracks as illustrated in Figure 16(a). The amplitudes of the emitted and reflected impulse, caused by cracks, are assessed in an A-scan plot as function of time, such as displayed in Figure 15(b).

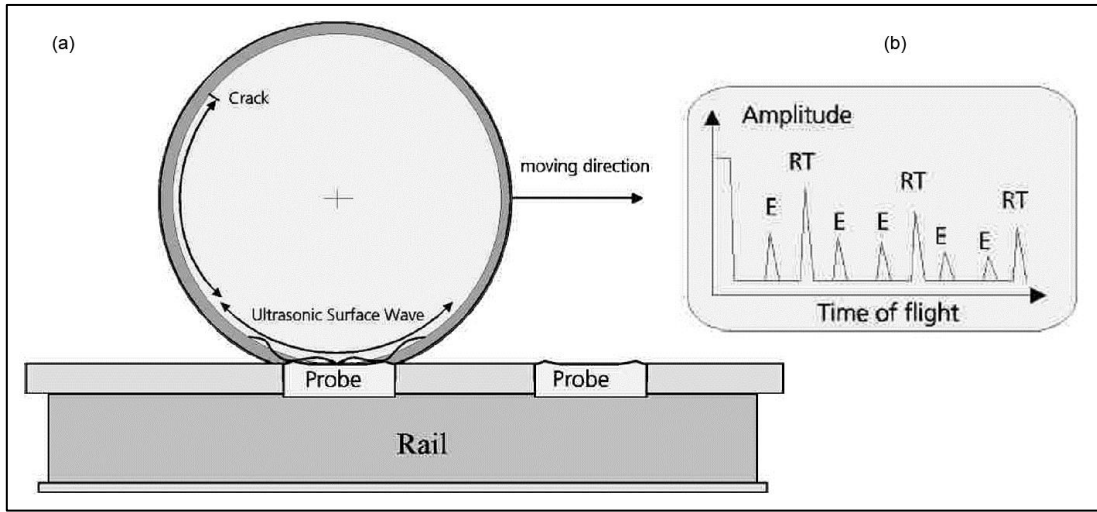


**Figure 15.** (a) Structure of two ultrasonic probes mounted on the specific rail (b) A-scan plot of a defective wheel.<sup>47</sup>

Brizuela *et al.* in<sup>48</sup> carried out a simulation and a laboratory test to evaluate the ability of Doppler effect in wheel fault detection. As illustrated in Figure 16 two piezoelectric transducers were mounted on a rail. The propagated monochromatic wave in the rail is reflected by the wheel-rail contact point. Relating to the train speed, the wheel-rail contact point is moving and the frequency of the propagated wave is shifted and calculated according to:

$$f_d = \frac{2\omega R}{c} f_s \quad (8)$$

In this equation the shifted frequency ( $f_d$ ), the frequency of the propagated signal ( $f_s$ ), the wheel radius ( $R$ ), the angular speed ( $\omega$ ), and the ultrasonic wave velocity ( $C$ ) are considered.

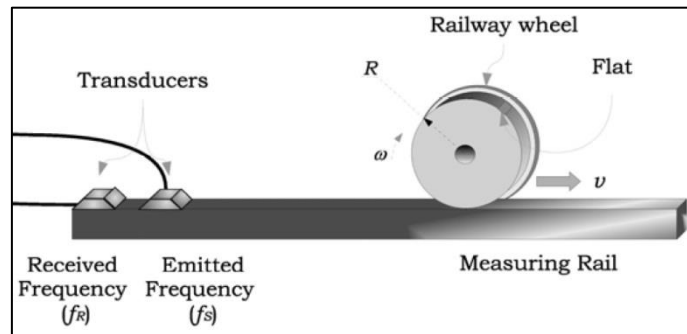


**Figure 16.** Configuration of a wheel-flat detector.<sup>48</sup>



Faults of the wheel tread change the frequency shift and are used for surface defect detection. The authors applied a time-frequency analysis and a high pass filter to process the acquired data. In spite of its capability for in-service application and whole circumference monitoring, this method needs special rails, constant and low speed movement. In addition, it cannot imply any information about the faults, except their occurrence. Then, they developed a method to evaluate the wheel flat features in <sup>49</sup>. The length and depth of the flat are obtained via a theoretical calculation that is fed by the period of ultrasound wave, which travels to the rail-wheel contact point. They assessed their method through a simulation and a laboratory investigation, but its limitation for real field application is maintained. Kenderian *et al.* in <sup>50</sup> assessed the capability of the combination of ultrasonic technique with Laser and capacitive air-coupled transducer for monitoring wheel defects. They used this hybrid method for detection of surface and sub-surface crack in wheel tread and flaws in the wheel flange. The position of the transducers, laser beam direction and their results are illustrated in Figure 17.

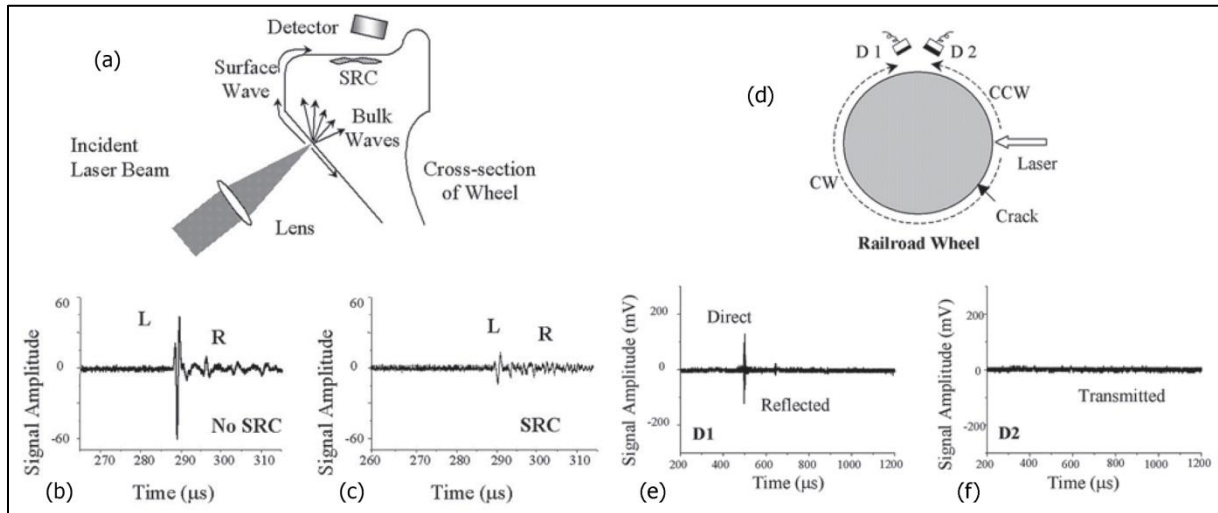


**Figure 17.** (a) Configuration of a sensor and wheel for surface and sub-surface monitoring, (b) the output of the monitoring system for a healthy wheel and (c) for a faulty wheel (Shattered rim cracks (SRC)), (d) configuration of sensors and wheel for wheel flange monitoring, (e) the results of D1 for monitoring of the faulty wheel, (f) the results of D2 for monitoring of the faulty wheel.<sup>50</sup>

**Vibration.** Bracciali and Cascini in <sup>51</sup> used an acceleration signal to sense the wheel flat and corrugation in wheel tread by comparing the results of energy and cepstrum analysis with the predetermined thresholds. The exerted energy from a wheel to the rail is dependent on the train speed, so they ran their tests with constant speed. Different positions and directions for six piezoelectric accelerometers were experienced and the best location (sensor 2 as displayed in Figure 18) was obtained.

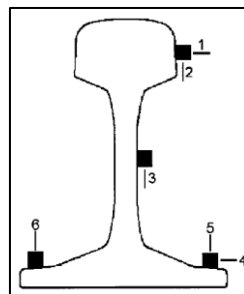


**Figure 18.** Different positions and directions for installing an accelerometer on the rail.<sup>51</sup>

Based on the repetitive trace of wheel flat, the power cepstrum is a very useful approach to find the echoes of the wheel flat in a noisy signal. This system detects the occurrence of the wheel flat in a bogie, however it is not able to identify the exact defective wheel.<sup>51</sup>

Skarlatos *et al.* in <sup>52</sup> applied fuzzy-logic method to diagnose the different levels of the wheel condition such as good, low damaged, faulty and dangerous. For achieving this purpose, the vibration amplitude value, the centre frequency band and the train velocity were used as three inputs, while the output was the condition of the train. In their field tests, the accelerometers were mounted on the rail according to position 5 in Figure 18. In addition, it was studied whether the vibration amplitude is a function of the train speed and frequency, or not. The vibration signals were measured at different train speeds and statistically analysed. As a result, it was concluded that the train speed and frequency have considerable effect on the vibration.

In Figure 19, an example of the measured signal is displayed and the result of an additional axle counter is presented at the top of the plot. It is noticeable that the measured acceleration signal could not directly refer to the number of axles passing the measurement point; therefore, it needs supplementary process. Belotti *et al.* in <sup>53</sup> exploited acceleration signals to sense the existence of wheel flats. In second step, they quantified the degree of damages using wavelet transform as a time–frequency processing approach. Knowing the type of train and consequently the distance between the axles, the train speed is calculated. Furthermore, they counted the train axles using handled data. Based on practical aspects, the wagons with faulty wheels are separated and planned for maintenance. Therefore, they concentrated on determining the bogie containing the wheel flat instead of detecting individual defective wheel. For these field measurements, the acceleration signals were collected by one sensor at different train speed from 10-100 km/h, with 10km/h interval.

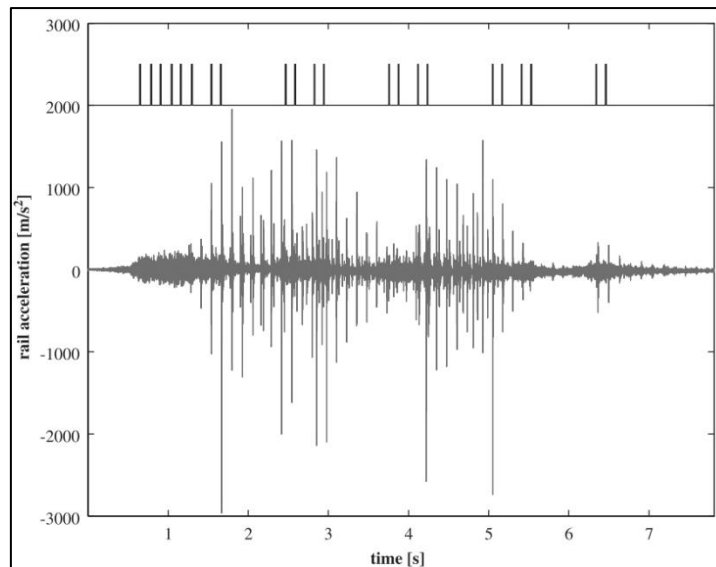


**Figure 19.** An example of the acquired acceleration signal.<sup>53</sup>

Shear-bridges, which are constructed by strain gauges, have a limited operational region so simultaneous interaction within faulty wheels and sensors is crucial. Converting the measured acceleration signal to the exerted impact force for overcoming this drawback was discussed in <sup>54</sup>. Lee and Chiu compared two methods to discover the relation between acquired track acceleration response and the magnitude of wheel impact force, inverse analysis method as a deconvolution technique, and root mean square method. Besides accelerometers, shear-bridges were also used for evaluating the results obtained in their field measurements. Inverse analysis method delivered good performance for computing the impact force beyond the operational region of the strain gauge. Typical examples of signals picked up by a shear-bridge and an accelerometer are given in Figure 20(a) and (b) respectively. Looking at the standard deviation of the impact force obtained by the shear-bridges in the calibration process, they concluded that shear-bridge measurements are not dependent on the train speed and load within their operational condition.



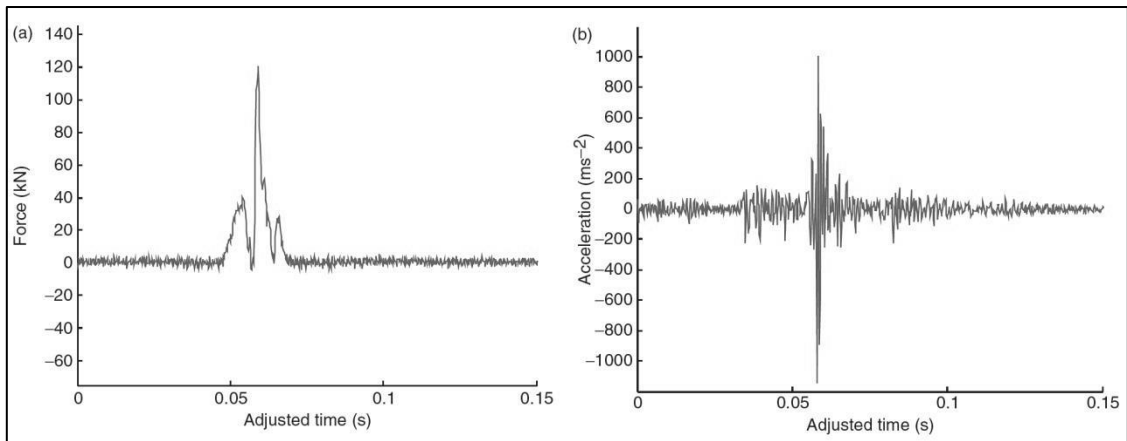


**Figure 20.** (a) Force signal measured by a shear-bridge and (b) acceleration signal measured by an accelerometer.<sup>54</sup>

**Acoustic Emission.** Thakkar *et al.* in <sup>55</sup> performed field and laboratory tests to measure the speed of the acoustic wave and the attenuation coefficient. Using these factors, an analytical acoustic emission model was built. They used the envelope of the root mean square of the signal as a comparison parameter between the emitted wheel-rail acoustic wave and the model to find the defect in the wheel-rail interaction area in the test rig. The structure of the test rig is displayed in Figure 21.

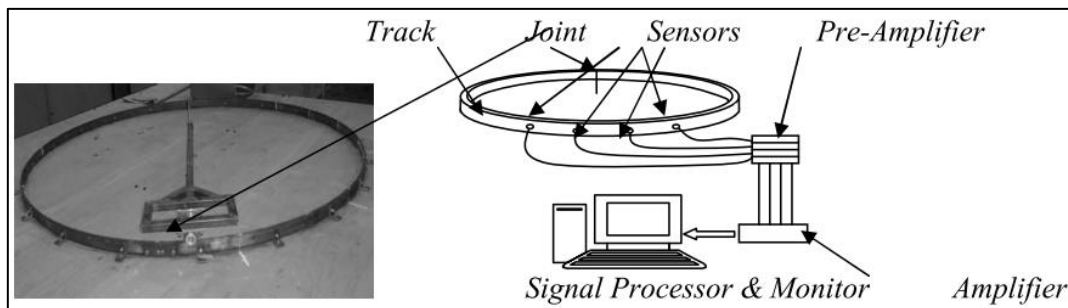


**Figure 21.** The structure of the acoustic test rig.<sup>55</sup>

They extended their scaled test rig experiments to wheel flat detection in <sup>56</sup>. They assessed the frequency and harmony of the acoustic wave propagated by defective wheel to diagnose the entity of wheel flat. This is built on the fact that the quantity, quality and position of the wheel flats change the features of the normal signal.

Wheel defects emit a periodic acoustic impulse regarding to the train speed and based on this consideration, recognition of a repetitive pattern in acoustic signal was discussed in <sup>57</sup>. For this purpose, Bollas *et al.* firstly applied a low pass filter on the acoustic waveform, which was measured by the sensors attached on the rail. Then the root mean square for the signal was calculated considering 40ms as the time window. The frequency spectrum of the acquired signal was obtained using a Fourier transform. In the last stage, the Harmonic Product Spectrum method determined the fundamental frequency that explains the entity of a repeated impact caused by a defect. In addition, they used Time Driven Data method for finding the wheel defect. They obtained the features of the acoustic signals of a normal train and compared them with the measured signals from defective train. The trend of these signals leads to the derivation of the presence of defects. In their assessments, the train speed was around 8-16 km/h. The ability of this method should be checked further for upper speeds and lower signal to noise ratio. Furthermore, these methods only indicate the existence of a wheel defect in the train and cannot determine yet the position of the faulty wheel and its severity.

**Lasers and high-speed cameras.** In <sup>58</sup> Yang *et al.* exploited lasers to emit light on the wheel surface and a high speed camera to catch the features of the wheel profile. This system can be mounted on normal rails and can be used for high-speed train up to 160km/h. The configuration of the monitoring system on the rail for decreasing the measurement noise is illustrated in Figure 22(a), and the captured profile curve in Figure 22(b). The comparison between the attained and reference profile leads to fault diagnosis. The main challenges in this research were noise cancellation and accurate recognition of wheel profile. Hence, the authors developed an image-tracking algorithm for acquiring the wheel profile.

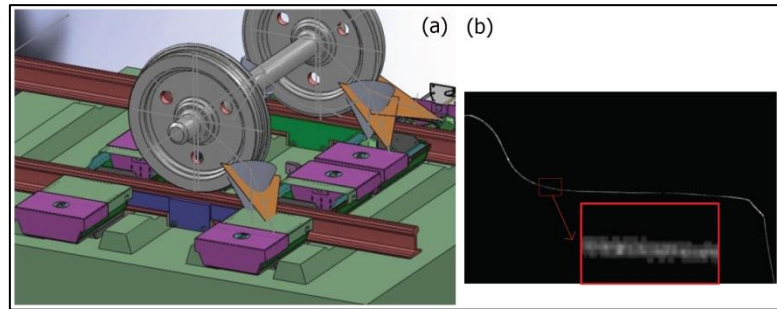


**Figure 22.** (a) The arrangement of the lasers and high-speed camera; (b) the captured wheel profile.<sup>58</sup>

## Discussion

Obviously, the monitoring systems follow different objectives and categorizing the literatures based on that can enhance the understanding of the state of the art approaches, and the research gap. Therefore, in the first part of this section, the objectives of the reviewed monitoring systems are discussed. In the second part, rail, train and sensor condition for an accurate and repeatable data acquisition is discussed. Finally, diagnosis and prognosis aspects in monitoring of railway wheel are considered.

### Measurement objective

**In-workshop inspection.** The available methods for monitoring the cracks of a railway wheel, based on their ability to sense the crack at different depths, can be classified into three main groups: surface cracks, sub-surface cracks, and the cracks in the rim and disk. Sub-surface cracks are induced by rolling contact fatigue, and are mostly at 3–5mm depth from the wheel surface.<sup>59</sup> Generally, the sub-surface cracks can be divided into two ranges: from surface to 5mm depth, and deeper cracks in the rim and disc. The techniques that are able to monitor the deeper cracks in wheel rim and disk are usually able to monitor sub-surface cracks as well. In-workshop inspection systems should be able to monitor the surface and sub-surface cracks with high accuracy. In Table 1, the available literature about in-workshop inspections based on the objective of the monitoring system is analysed.

**Table 1.** The objectives of the monitoring systems for in-workshop inspections

Objective of monitoring	Technique or sensor	Assessment level
Surface crack	Magnetic technique	Test rig <sup>26</sup>
Sub-surface crack	Ultrasonic technique	Test rig <sup>19</sup>
	Magnetic technique	Test rig <sup>24, 25</sup>
Cracks in wheel rim and disk	Ultrasonic technique	Field measurement <sup>18, 21, 22</sup>
	Infrared camera	Test rig <sup>23</sup>
Contact pressure distribution	Ultrasonic technique	Test rig <sup>17, 19, 20</sup>
		Simulation, <sup>20</sup>

The ultrasonic technique is the only available method used so far in field measurements. The magnetic technique and the infrared camera have been used in test rigs and can be potentially used in field measurements.

***In-service and on-board inspection.*** The variety of trains and wheel types, difficulty of the installation, and issues in maintaining the mounted sensors, restrict the on-board inspection of in-service monitoring. As it is clear in Table 2, flange contact, surface defects and derailment coefficient are the objectives of on-board monitoring systems. Furthermore, many research works were implemented in simulation and/or test rigs, while field measurements are scarce. As a result, on-board monitoring as an aspect of wheel condition monitoring has had, and still has, many complications waiting to be overcome.

**Table 2.** The objectives of the monitoring systems for in-service and on-board inspections

Objective of monitoring	Technique or sensor	Assessment level
<b>Flange contact</b>	Ultrasonic technique	Test rig - full-scale <sup>30</sup>
		Simulation <sup>30</sup>
<b>Surface defects</b>	Acoustic technique	Test rig - full-scale <sup>31</sup>
		Simulation <sup>31, 32</sup>
	Vibration technique	Test rig - scale test <sup>32, 33</sup>
		Simulation <sup>34</sup>
<b>Derailment coefficient</b>	Magnetic technique	Test rig - full-scale <sup>28</sup>
		Simulation <sup>28, 29</sup>
		Field measurement <sup>28, 29</sup>

***In-service and wayside inspection.*** In-service wayside inspection covers the most common wheel monitoring systems. According to Table 3, wayside inspection can be divided into two main groups: train identification, and wheel defect detection. For an applicable monitoring and perfect processing, the train identification is necessary. Axle counting, train speed and acceleration, dynamic and static load and ambient temperature are some features, which are included in the setup of such a system.

**Table 3.** The objectives of the monitoring systems for in-service and wayside inspections

Objective of monitoring	Technique or sensor	Assessment level
<b>Surface defects</b>	Strain gauges	Simulation <sup>60</sup>
		Field measurement <sup>60, 38</sup>
	Fibre Bragg Grating sensor	Field measurement <sup>10, 40, 44, 45, 61</sup>
	Ultrasonic technique	Simulation <sup>48</sup>
		Test rig <sup>47, 48</sup>
		Field measurement <sup>47</sup>
	Laser-Air Hybrid Ultrasonic Technique	Test rig <sup>50</sup>
	Vibration technique	Field measurement <sup>51, 52, 53, 54</sup>
	Acoustic technique	Simulation <sup>55</sup>
		Test rig <sup>55, 56</sup>
Field measurement <sup>55, 57</sup>		
<b>Surface defects quantification</b>	Fibre Bragg Grating sensor	Field measurement <sup>45</sup>
	Ultrasonic technique	Simulation <sup>49</sup>
		Test rig <sup>49</sup>

	Vibration technique	Field measurement <sup>53</sup>
<b>Sub-surface defects</b>	Strain gauges	Field measurement <sup>38</sup>
	Laser-Air Hybrid Ultrasonic Technique	Test rig <sup>50</sup>
<b>Steering ability</b>	Strain gauges	Field measurement <sup>6, 39</sup>
<b>Derailment coefficient</b>	Fibre Bragg Grating sensor	Field measurement <sup>42, 40, 46</sup>
	Piezoelectric Sensing Technology	Field measurement <sup>62</sup>
<b>Wheel profile parameters</b>	laser and high speed camera	Field measurement <sup>39, 58</sup>
<b>Train speed</b>	Fibre Bragg Grating sensor	Field measurement <sup>41, 44</sup>
	Vibration technique	Field measurement <sup>53</sup>
<b>Train acceleration</b>	Fibre Bragg Grating sensor	Field measurement <sup>44</sup>
<b>Axle counting</b>	Fibre Bragg Grating sensor	Field measurement <sup>43, 44</sup>
	Vibration technique	Field measurement <sup>53</sup>
<b>Dynamic load</b>	Fibre Bragg Grating sensor	Field measurement <sup>44, 45</sup>
<b>Static load (Weight of train)</b>	Fibre Bragg Grating sensor	Field measurement <sup>45, 40</sup>
<b>Train type identification</b>	Fibre Bragg Grating sensor	Field measurement <sup>44</sup>
<b>Ambient Temperature</b>	Fibre Bragg Grating sensor	Field measurement <sup>44</sup>

For surface defects detection, Fibre Bragg Grating sensor has very suitable output. Tam et al. mentioned several advantages of FBG sensors for railway applications<sup>41</sup>:

- Electromagnetic immunity; conventional strain gauges are affected by electromagnetic fields induced by high voltage overhead power lines.
- Ability of fabricating numerous sensors inside a fibre;
- Long conduction distance for distant detecting;
- Innate ability for self-referencing; FBG interrogator measures the wavelength change, therefore the measured value is an absolute parameter;
- Resolving the recalibration or re-initialization problem

Adding to these benefits, there are other factors cited in the literature such as:

- low cost and easy installation<sup>45</sup>;
- immediate time response, reliability, durability<sup>40</sup>;
- compact size, independence from electric power in the measurement point<sup>10</sup>;
- great accuracy and sensitivity, stability in spite of ambient temperature change, corrosion resistance<sup>46</sup>;
- ability of using only one end of the fibre for interrogating the data<sup>41</sup>.

In recent years, due to increasing train speeds and axle loads, wheel-rail interaction and consequently wheel-rail deterioration have changed. Hence, the wear of wheels as a dominant reason of their damage has been altered to fatigue.<sup>38</sup> This shifts the defects from surface to sub-surface; for this case, the wayside methods have not been developed well. According to Table 3, despite sufficient growth in surface defect detection by means of various techniques, sub-surface defect detection is still immature. Hence, additional research for extending the wayside system for monitoring sub-surface defects is an open challenge.

### ***Measurement conditions***

For an accurate and repeatable data acquisition, considering some settings during the measurement stage is necessary. The measurement condition can be described by: a healthy rail for installing the sensor, a curved track for measuring the flange contact and lateral force, a straight and horizontal track for vertical force, a convenient resolution for sensors (sample frequency), also the number and configuration of sensor array.

For example, in <sup>43</sup> and <sup>44</sup> different positions for mounting the sensors were assessed. Wei *et al.* <sup>43</sup> implemented an ANSYS analysis and laboratory test. Their results showed that the maximum deflection would be on the head and foot of the rail in case of longitudinal sensor. Details of the position of four longitudinal FBG sensors and three vertical FBG sensors are described in Figure 23.

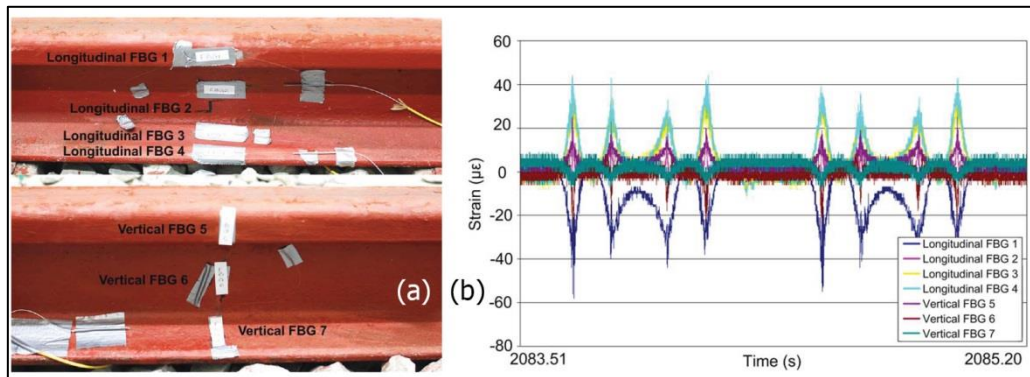


**Figure 23.** (a) Four longitudinal and three vertical FBG sensor mounted on the rail, (b) results of four times measurement of strain by means of mounted sensors.<sup>43</sup>

In addition, the effects of some factors of the rail, train and sensor should be considered, such as:

- Rail: different types of rail and profile, the sleeper and ballast properties;
- Train: type, speed, acceleration, deceleration, axle load, moving direction and wheel sizes;
- Sensor: the methods of installation, calibration factor, the measurement range of sensor, temperature change, and the signal to noise ratio.

### ***Diagnosis and Prognosis approaches***

Based on <sup>7</sup>, diagnosis and prognosis are two critical key concept in condition-based maintenance. In diagnosis, the current condition is considered for maintenance decision making; in the prognostic approach, detecting the deterioration over time, and predicting the future condition and remaining useful life are desired. In diagnostic approach, usually a deviation over a predetermined threshold is considered; instead, in prognostic, very tiny deviations from the normal condition are sensed. Therefore, sensitivity and accuracy of the measurement is a determinative parameter for prognosis.

Wheel defect detection can be categorized into these levels:

- 1- Detection of the train with one or more defective wheels;
- 2- Detection of the exact bogie with one or more defective wheels;
- 3- Detection of the exact defective wheel;
- 4- Quantification of the defect of the defective wheel;
- 5- Quantification of the condition of all wheels of the train;
- 6- Prognosis of the condition of all wheels of the train.

Selecting an adequate data acquisition system and processing method for each level depends on the maintenance strategy. Therefore, the quality of the data acquisition system should be assessed according to its target; hence, general comparison between different techniques is not sufficient.

In general, diagnosis is a more common approach than prognosis; in particular, this is the case also in the railway industry. All papers reviewed here worked on diagnosis of defects, with the exception of <sup>38</sup> and <sup>10</sup> that showed the evolution of wheel defects over time. Hence, attention to the prognostic approach for predicting the future wheel defects is an open direction for research.

**Normalizing the data.** In prognosis, comparing the data over time, finding the deterioration pattern and consequently building a model for predicting the future condition are required. Therefore, normalizing the measured data for eliminating the effects of the various measurement conditions is essential.

A research group in Hong Kong Polytechnic University in <sup>61</sup>, <sup>40</sup> and <sup>10</sup> introduced a condition index for normalization of the measured data. In <sup>61</sup> and <sup>40</sup> they mentioned the train speed, vibration frequency and vibration magnitude as factors of the condition index. They only compared the obtained condition index of faulty and healthy wagons in a train without discussing the way of calculating this index. Wei et al. in <sup>10</sup> proposed a condition index (CI) based on average amount of the strain changes ( $\bar{\varepsilon}$ ) and train speed (V) for in-service and real-time evaluation of the wheels condition as formulated in the equation 9:

$$CI = \frac{\bar{\varepsilon}}{V} \times A \quad (9)$$

In this equation, A is a scaling factor. They proved their method by field investigation of 29 passenger trains. Figure 24 displays the progress of the condition index during a period of ten months assessment. The considerable decrease in condition index after 60<sup>th</sup> day is because of re-profiling.

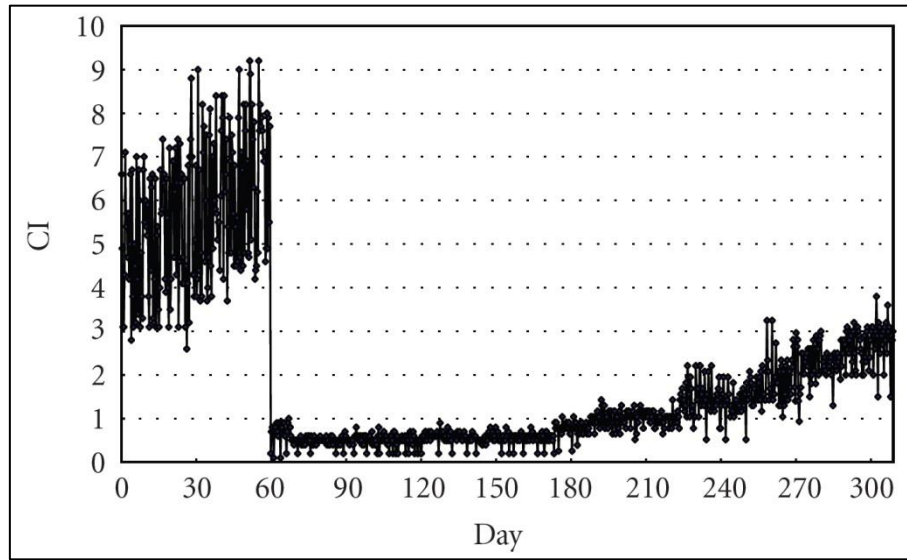


**Figure 24.** Evolution of the condition index over time.<sup>10</sup>

As stated by Ver in <sup>63</sup>, wheel-rail interaction is affected by train speed; exceeding a specific threshold speed leads to wheel-rail separation in a faulty interface. Hence, considering the train speed for indirect monitoring methods that are based on wheel-rail interaction is important. On the other hand, according to <sup>53</sup>, the relationship between the defect severity (such as length of wheel-flat) and exerted impact force is not linear. Therefore, these phenomena should be considered in the normalizing stage.

Filigrano *et al.* in <sup>45</sup> described the impact force as the sum of the static load of train and a dynamic overload. They supposed that this dynamic overload is a partially stochastic quantity, which is a function of the train velocity. Moreover, they estimated the average value of the dynamic overload 21% and 14.5% of the static load at 300 and 200 km/h respectively. Stratman *et al.* in <sup>38</sup> used two methods to normalize the measured impact force and to eliminate the effect of the train weight. They gathered the vertical and lateral forces at 16 points per rail. First, the average of the measured forces was calculated, then differences between the maximum value and the average were determined, which was called “dynamic impact load”. In the second method, the ratio of the maximum value and the average was calculated as a “ratio”.

$$\text{Dynamic impact load} = \text{maximum impact force} - \text{average force} \quad (10)$$

$$\text{Ratio} = \frac{\text{maximum impact force}}{\text{average force}} \quad (11)$$

They are considered “semi-normalized impact forces” because they eliminate the influence of the train weight on the measured impact, leaving out the effect of the train speed.

In <sup>60</sup> a wheel impact load detector based on 11 strain gauges was used to evaluate the effect of a variety of wheel defects on the vertical dynamic contact force. These field experiments were performed in the range of 30-100 km/h train speeds with two dissimilar axle loads. The effects of train speed on impact force and rail bending moment were assessed on measured data from Svealandsbanan (2000) (Figure 25). In that test, the train was loaded and the measured data were compared with the numerical simulated data. The fitted curve shows a local maximum at a train speed of 40 km/h.

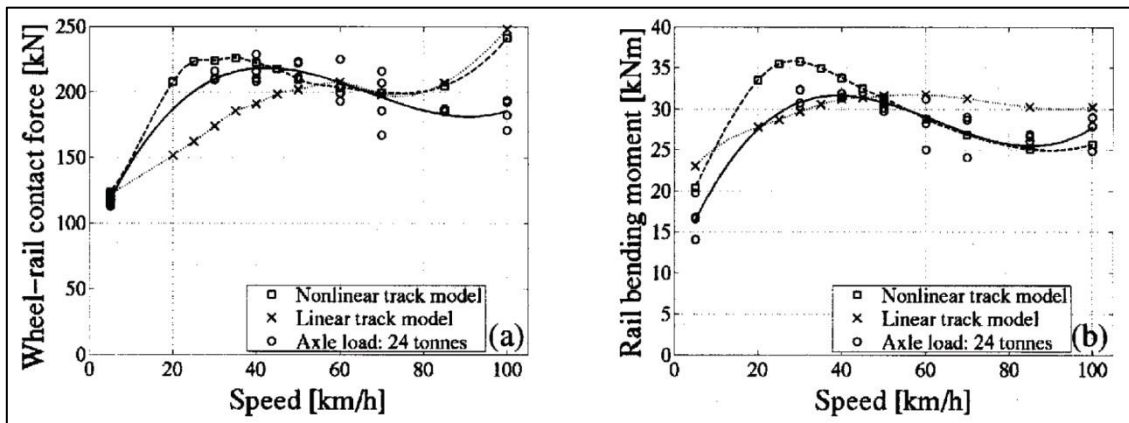


**Figure 25.** Comparison of the measured and simulated data at different train speeds with a faulty wheel-set in (a) maximum vertical impact force and (b) maximum rail bending moment.<sup>60</sup>

In Figure 26, the measured data from Sannahed (1997) for a wheel flat and long local defective wheel (30–50 cm defect with a depth of 3-5 mm) at different train speeds and load conditions are displayed. It is noticeable that in Figure 26(a), local maximum is at 40 km/h. In addition, it is clear that wheel-rail contact force for long local defective wheels has an approximately linear relation with train speed.

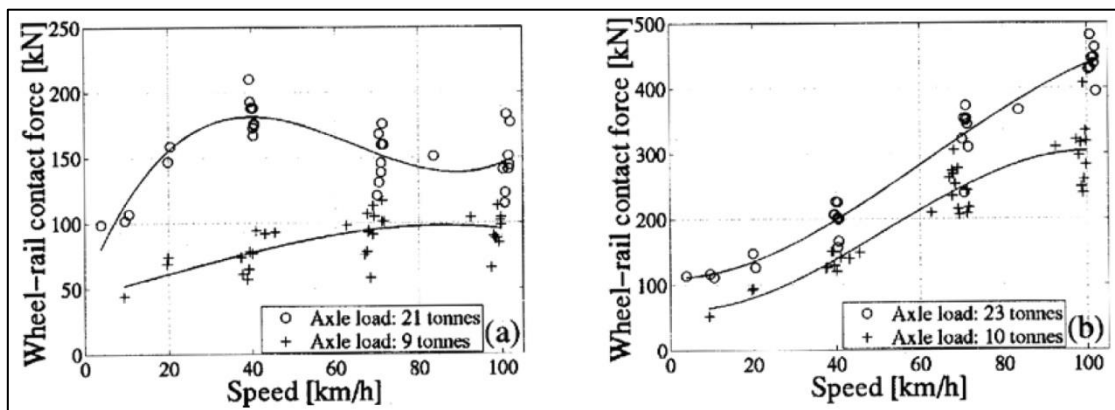


**Figure 26.** Loaded wagon (o) and empty wagons (+) for: (a) wheel-set with a 100mm wheel-flat and (b) faulty wheel with a 0.5m long local defect.<sup>60</sup>

Another research reviewed in <sup>2</sup> demonstrates the effects of train speed and defect severity on the impact load. In Figure 27, it is displayed that the length growth of the wheel flat increases the impact load. It is remarkable, that increasing the train speed generally increases the impact load, except at some specific wheel flat lengths. As a result, train speed, train weight (axle load) and wheel defect types and severity are the main factors that influence

the impact load. The comparison between Figure 27 and 25, 26 shows that other than the parameters stated above, also their different combinations influence the impact load as well. Therefore, this should be considered in the data acquisition stage.

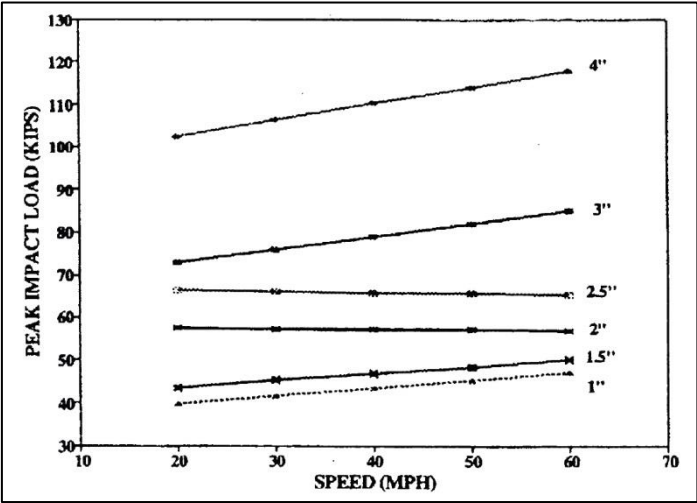


**Figure 27.** Measured impact loads for different lengths of the wheel flat with increase in train speed. (1 kip = 4.45 KN; 1 mile/h = 1.609 km/h and 1 inch = 25.4 mm).<sup>2</sup>

**Conclusion**

The assessment of the papers studied shows that wheel monitoring is an active area of research, as plotted in Figure 28. While the railway network is distributed all over the world and several commercial products for condition monitoring exist in this field <sup>37</sup>, more attention is required to develop new advanced monitoring systems.

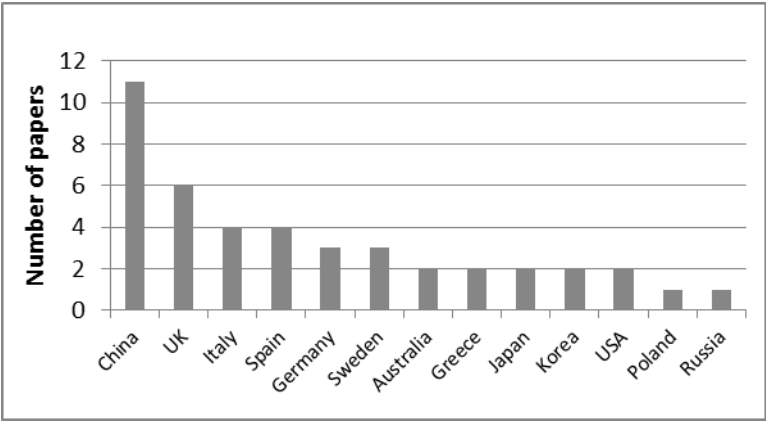


**Figure 28.** Active countries in developing wheel monitoring system for literature published from 2003 to 2015.

The main conclusions of the analysis are reported here. In-workshop monitoring systems have a specific role in periodic inspection. Hence, further research on increasing the accuracy and decreasing the time spent on multiple inspections is required. In addition, developing wayside systems for monitoring sub-surface defects is still necessary. Furthermore, more simulations and measurements are required to evaluate the effects of train speed, train weight and the type and severity of surface defects reflected in the wayside measurement data.

Using a prognostic method for predicting future failures and optimizing the maintenance plan can lead to improvements in efficiency. To move from a diagnostic to a prognostic approach, it is vital to assess the effect of different parameters in various measurement conditions. Using multiple sensors and multiple stations for data



acquisition and related data fusion can be an important stage in the development of the wheel condition monitoring system.

## References

1. Chong SY, Lee J-R, Shin H-J. A review of health and operation monitoring technologies for trains. *Smart Struct Syst* 2010; 6: 1079–1105.
2. Nielsen JCO, Johansson A. Out-of-round railway wheels—a literature survey. *Proc Inst Mech Eng Part F J Rail Rapid Transit* 2000; 214: 79–91.
3. Tinga T. Application of physical failure models to enable usage and load based maintenance. *Reliab Eng Syst Saf* 2010; 95: 1061–1075.
4. Fröhling RD. Wheel/rail interface management in heavy haul railway operations—applying science and technology. *Veh Syst Dyn* 2007; 45: 649–677.
5. Lin J, Asplund M, Parida A. Reliability analysis for degradation of locomotive wheels using parametric Bayesian approach. *Qual Reliab Eng Int* 2014; 30: 657–667.
6. Palo M, Schunnesson H, Kumar U, et al. Rolling stock condition monitoring using wheel/rail forces. *Insight - Non-Destructive Test Cond Monit* 2012; 54: 451–455.
7. Jardine AKS, Lin D, Banjevic D. A review on machinery diagnostics and prognostics implementing condition-based maintenance. *Mech Syst Signal Process* 2006; 20: 1483–1510.
8. Lee J, Wu F, Zhao W, et al. Prognostics and health management design for rotary machinery systems—Reviews, methodology and applications. *Mech Syst Signal Process* 2014; 42: 314–334.
9. Ngigi RW, Pislaru C, Ball A, et al. Modern techniques for condition monitoring of railway vehicle dynamics. *J Phys Conf Ser* 2012; 364: 012016.
10. Wei C, Xin Q, Chung WH, et al. Real-time train wheel condition monitoring by Fiber Bragg Grating sensors. *Int J Distrib Sens Networks* 2012; 2012: 1–7.
11. Vries M de. *Just in time delivery of wheel sets*. Master Thesis, Delft University of Technology, The Netherlands, 2013.
12. Ahmad R, Kamaruddin S. An overview of time-based and condition-based maintenance in industrial application. *Comput Ind Eng* 2012; 63: 135–149.
13. Veldman J, Wortmann H, Klingenberg W. Typology of condition based maintenance. *J Qual Maint Eng* 2011; 17: 183–202.
14. Ward CP, Weston PF, Stewart EJC, et al. Condition monitoring opportunities using vehicle-based sensors. *Proc Inst Mech Eng Part F J Rail Rapid Transit* 2011; 225: 202–218.
15. Barke D. Structural health monitoring in the railway industry: a review. *Struct Heal Monit* 2005; 4: 81–93.
16. Drinkwater BW, Wilcox PD. Ultrasonic arrays for non-destructive evaluation: A review. *NDT E Int* 2006; 39: 525–541.

17. Pau M. Ultrasonic waves for effective assessment of wheel-rail contact anomalies. *Proc Inst Mech Eng Part F J Rail Rapid Transit* 2005; 219: 79–90.
18. Pohl R, Erhard A, Montag H-J, et al. NDT techniques for railroad wheel and gauge corner inspection. *NDT E Int* 2004; 37: 89–94.
19. Pau M, Leban B, Baldi A. Simultaneous subsurface defect detection and contact parameter assessment in a wheel–rail system. *Wear* 2008; 265: 1837–1847.
20. Marshall MB, Lewis R, Dwyer-Joyce RS, et al. Experimental characterization of wheel-rail contact patch evolution. *J Tribol* 2006; 128: 493.
21. Peng C, Gao X, Wang L, et al. Automatic railway wheelset inspection system by using ultrasonic technique. In: Fan K-C, Song M, Lu R-S (eds) *Proceedings of SPIE - The International Society for Optical Engineering*. 2011, p. 83212C.
22. Gao X, Wang Z, Peng C, et al. Research on automatic defect localization for ultrasonic normal probe detection on railway wheel. In: Fan K-C, Song M, Lu R-S (eds) *Seventh International Symposium on Precision Engineering Measurements and Instrumentation*. 2011, p. 83212X.
23. Verkhoglyad a. G, Kuropyatnik IN, Bazovkin VM, et al. Infrared diagnostics of cracks in railway carriage wheels. *Russ J Nondestruct Test* 2008; 44: 664–668.
24. Kwon SJ, Seo JW, Lee DH, et al. Detection of sub-surface crack in railway wheel using a new sensing system. In: Wu HF (ed) *Proceedings of SPIE - The International Society for Optical Engineering*. 2011, p. 79833A–79833A–5.
25. Żurek ZH. Magnetic monitoring of the fatigue process of the rim material of railway wheel sets. *NDT E Int* 2006; 39: 675–679.
26. Hwang J, Lee J, Kwon S. The application of a differential-type Hall sensors array to the nondestructive testing of express train wheels. *NDT E Int* 2009; 42: 34–41.
27. Hwang JS, Lee JY. Magnetic images and NDT of the express train wheel using a high speed scan-type magnetic camera. *Key Eng Mater* 2009; 417-418: 169–172.
28. Matsumoto A, Sato Y, Ohno H, et al. A new measuring method of wheel–rail contact forces and related considerations. *Wear* 2008; 265: 1518–1525.
29. Matsumoto A, Sato Y, Ohno H, et al. Actual states of wheel/rail contact forces and friction on sharp curves – Continuous monitoring from in-service trains and numerical simulations. *Wear* 2014; 314: 189–197.
30. Dwyer-Joyce RS, Yao C, Lewis R, et al. An ultrasonic sensor for monitoring wheel flange/rail gauge corner contact. *Proc Inst Mech Eng Part F J Rail Rapid Transit* 2013; 227: 188–195.
31. Frankenstein B, Hentschel D, Pridoehl E, et al. Hollow shaft integrated health monitoring system for railroad wheels. In: Meyendorf N, Baaklini GY, Michel B (eds) *Proceedings of SPIE - The International Society for Optical Engineering*. 2005, pp. 46–55.
32. Liang B, Iwnicki SD, Zhao Y, et al. Railway wheel-flat and rail surface defect modelling and analysis by time–frequency techniques. *Veh Syst Dyn* 2013; 51: 1403–1421.
33. Liang B, Iwnicki S, Ball A, et al. Adaptive noise cancelling and time–frequency techniques for rail surface defect detection. *Mech Syst Signal Process* 2015; 54-55: 41–51.

34. Jia S, Dhanasekar M. Detection of rail wheel flats using wavelet approaches. *Struct Heal Monit* 2007; 6: 121–131.
35. Partington W. Wheel impact load monitoring. *Proc ICE - Transp* 1993; 100: 243–245.
36. Asplund M, Palo M, Famurewa S, et al. A study of railway wheel profile parameters used as indicators of an increased risk of wheel defects. *Proc Inst Mech Eng Part F J Rail Rapid Transit* 2014.
37. Brickle B, Morgan R, Smith E, et al. *Identification of existing and new technologies for wheelset condition monitoring*. Report for the Rail Safety and Standards Board (RSSB). Report no. T607, 2008.
38. Stratman B, Liu Y, Mahadevan S. Structural health monitoring of railroad wheels using wheel impact load detectors. *J Fail Anal Prev* 2007; 7: 218–225.
39. Palo M, Galar D, Nordmark T, et al. Condition monitoring at the wheel/rail interface for decision-making support. *Proc Inst Mech Eng Part F J Rail Rapid Transit* 2014; 228: 705–715.
40. Lai CC, Kam JCP, Leung DCC, et al. Development of a Fiber-Optic Sensing System for Train Vibration and Train Weight Measurements in Hong Kong. *J Sensors* 2012; 2012: 1–7.
41. Tam HY, Liu SY, Guan BO, et al. Fiber Bragg Grating sensors for structural and railway applications. In: Rao Y-J, Kwon OY, Peng G-D (eds) *Proceedings of SPIE - The International Society for Optical Engineering*. 2005, pp. 85–97.
42. Lee K, Lee K, Ho S. Exploration of using FBG sensor for derailment detector. *WSEAS Trans Top Syst* 2004; 3: 2433–2439.
43. Chu-liang Wei, Chun-cheung Lai, Shun-ye Liu, et al. A Fiber Bragg Grating sensor system for train axle counting. *IEEE Sens J* 2010; 10: 1905–1912.
44. Filograno ML, Corredera Guillen P, Rodriguez-Barrios A, et al. Real-time monitoring of railway traffic using Fiber Bragg Grating sensors. *IEEE Sens J* 2012; 12: 85–92.
45. Filograno ML, Corredera P, Rodriguez-Plaza M, et al. Wheel flat detection in high-speed railway systems using Fiber Bragg Gratings. *IEEE Sens J* 2013; 13: 4808–4816.
46. Pan J, Li W, Dai X. Train overload and unbalanced load detection based on FBG gauge. In: Yang M, Wang D, Rao Y-J (eds) *Proceedings of SPIE - The International Society for Optical Engineering*. 2013, p. 89242D.
47. Salzburger HJ, Schuppmann M, Li W, et al. In-motion ultrasonic testing of the tread of high-speed railway wheels using the inspection system AUROPA III. *Insight - Non-Destructive Test Cond Monit* 2009; 51: 370–372.
48. Brizuela J, Ibañez A, Nevado P, et al. Railway wheels flat detector using Doppler effect. *Phys Procedia* 2010; 3: 811–817.
49. Brizuela J, Fritsch C, Ibañez A. Railway wheel-flat detection and measurement by ultrasound. *Transp Res Part C Emerg Technol* 2011; 19: 975–984.
50. Kenderian S, Djordjevic BB, Cerniglia D, et al. Dynamic railroad inspection using the laser-air hybrid ultrasonic technique. *Insight - Non-Destructive Test Cond Monit* 2006; 48: 336–341.
51. Bracciali A, Cascini G. Detection of corrugation and wheel flats of railway wheels using energy and cepstrum analysis of rail acceleration. *Proc Inst Mech Eng Part F J Rail Rapid Transit* 1997; 211: 109–116.

52. Skarlatos D, Karakasis K, Trochidis A. Railway wheel fault diagnosis using a fuzzy-logic method. *Appl Acoust* 2004; 65: 951–966.
53. Belotti V, Crenna F, Michelini RC, et al. Wheel-flat diagnostic tool via wavelet transform. *Mech Syst Signal Process* 2006; 20: 1953–1966.
54. Lee ML, Chiu WK. Determination of railway vertical wheel impact magnitudes: field trials. *Struct Heal Monit* 2007; 6: 49–65.
55. Thakkar N a., Steel J a., Reuben RL, et al. Monitoring of rail-wheel interaction using acoustic emission (AE). *Adv Mater Res* 2006; 13-14: 161–168.
56. Thakkar N a., Steel J a., Reuben RL. Rail-wheel contact stress assessment using acoustic emission: a laboratory study of the effects of wheel flats. *Proc Inst Mech Eng Part F J Rail Rapid Transit* 2012; 226: 3–13.
57. Bollas K, Papasalouros D, Kourousis D, et al. Acoustic emission monitoring of wheel sets on moving trains. *Constr Build Mater* 2013; 48: 1266–1272.
58. Yang K, Ma L, Gao X, et al. Profile parameters of wheelset detection for high speed freight train. In: Othman M, Senthilkumar S, Yi X (eds). 2012, p. 83341W–83341W–6.
59. Mutton PJ, Epp CJ, Dudek J. Rolling contact fatigue in railway wheels under high axle loads. *Wear* 1991; 144: 139–152.
60. Johansson A, Nielsen JO. Out-of-round railway wheels—wheel—rail contact forces and track response derived from field tests and numerical simulations. *Proc Inst Mech Eng Part F J Rail Rapid Transit* 2003; 217: 135–146.
61. Ho SL, Lee KK, Lee KY, et al. A comprehensive condition monitoring of modern railway. In: *IET International Conference on Railway Condition Monitoring*. IEE, 2006, pp. 125–129.
62. Song Y, Du YL, Sun BC. Study on wheel/rail interaction force real-time monitoring method based on piezoelectric sensing technology. *Adv Mater Res* 2009; 79-82: 7–10.
63. Vér IL, Ventres CS, Myles MM. Wheel/rail noise—Part III: Impact noise generation by wheel and rail discontinuities. *J Sound Vib* 1976; 46: 395–417.